Photochemical Generation and Matrix-Isolation Detection of Dimethylvinylidene

Sasha C. Reed,[‡] Gregory J. Capitosti,[§] Zhendong Zhu,[⊥,†] and David A. Modarelli*[,§]

Departments of Chemistry, Knight Chemical Laboratory, The University of Akron, Akron, Ohio 44325-3601, Colgate University, Hamilton, New York 13346, and The Ohio State University, Columbus, Ohio 43210

dam@chemistry.uakron.edu.

Received October 10, 2000

We report the spectroscopic characterization of dimethylvinylidene, $(CH_3)_2C{=}C{:}$, generated within an argon matrix at 14 K from a bisperoxyester precursor. The carbene was identified by comparison of the experimental IR spectrum with vibrational frequencies computed at the B3LYP/6-31G(d) level. Chemical trapping of the carbene within a 9% CO/Ar matrix to form dimethylpropadienone supports this analysis. Additional products produced during photolysis were identified by comparison to the appropriate computed vibrational frequencies. The potential energy surface of dimethylvinylidene and its intramolecular rearrangement products, 2-butyne and methylcyclopropene, were also investigated computationally at the B3LYP/6-31G(d) level. A spin-state analysis of this carbene using a variety of computational methods (CCSD(T), B3LYP, MP2) indicates the singlet state is more stable than the triplet by ∼45 kcal mol^{-1}. We anticipate the bisperoxyester precursor used here will be a convenient and general way for initiating future studies of alkylvinylidenes under matrix-isolation conditions.

Introduction

Aryl, alkyl, and halocarbenes are by now well characterized by theory and spectroscopic (UV−vis, IR, EPR, time-resolved) techniques.[1] The spectroscopy of alkylvinylidenes ($R_2C{=}C{:}$, i.e., **1**) is not as well understood, although the solution-phase chemistry of alkylvinylidenes is relatively well established and is typical of carbene chemistry.[2] Considering the important role these reactive species may play in the interstellar medium,[3] the lack of spectroscopic evidence for alkylvinylidenes is of current interest in physical organic chemistry.

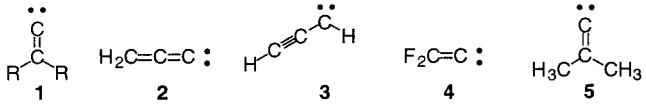

1 **2** **3** **4** **5**

The theoretical debate of whether **1** (R = H) actually exists as a bound state is substantial.[4] The highest level calculations (CCSD(T)/TZ+2P, EOM-CCSD/TZ2P) to date from Schaefer's and Stanton's groups[4,5] indicate the barrier height for isomerization to acetylene to be ∼3 kcal mol^{-1}. Thus, vinylidene **1** is predicted to exist as a reactive intermediate. Schaefer[4,6] and others[7,8] have also computationally explored the energies and structures of several substituted vinylidenes. Spin-state analyses indicate the singlet states in all cases are more stable than the corresponding triplet states by a substantial amount (∼35−50 kcal mol^{-1}).[4] The large difference in spin-state energies is not surprising considering the doubly occupied orbital in the $^1A_1$ singlet is sp-hybridized in origin. Promotion of an electron to the nonbonding and higher energy carbene p-orbital is unfavorable.[9]

Vinylidene and its deuterated and fluorinated analogues have been indirectly detected by gas-phase photoelectron-detachment[9] and dispersed-fluorescence spectroscopies.[10] From Lineberger's work[9] the vibrational spectrum of **1** was determined and the barrier to rearrangement to acetylene estimated from the 2←0 CH_2-rock mode to be ∼1.3 kcal mol^{-1}. The lifetime of (R=H) **1** was also estimated to be ∼0.04−0.2 ps on the basis of line-broadening simulations. The enthalpy of this reaction has been deduced[9,10] to be exothermic by ∼41−45 kcal mol^{-1}.

Recently, matrix isolation has been used to isolate and study two vinylidenes. Maier et al.[11] irradiated cyclopropenylidene in an argon matrix to isolate a mixture of

[§] The University of Akron.
[‡] Colgate University.
[⊥] The Ohio State University.
[†] Current Address: Institute of Cognitive and Computational Science, Georgetown University Medical Center, Washington, DC 20007.

(1) Platz, M. S. *Kinetics and Spectroscopy of Carbenes and Biradicals*; Plenum Press: New York, 1990.
(2) Jones, M., Jr.; Moss, R. A. *Carbenes*; Krieger Publishing Co.: Malabar, FL, 1983.; Kirmse, W. *Carbene Chemistry*; Academic Press: New York, 1971.
(3) Vrtilek, J. M.; Gottlieb, C. A.; Gottlieb, E. W.; Killian, T. C.; Thaddeus, P. *Astrophys. J.* **1990**, *364*, L53. Cernicharo, J.; Gottlieb, C. A.; Guélin, M.; Killian, T. C.; Paubert, G.; Thaddeus, P.; Vrtilek, J. M. *Astrophys. J.* **1991**, *368*, L39.
(4) Gallo, M. M.; Hamilton, T. P.; Schaefer, H. F. *J. Am. Chem. Soc.* **1990**, *112*, 7714−8719.
(5) Stanton, J. F.; Gauss, J. *J. Chem. Phys.* **1994**, *101*, 3001−3005.
(6) (a) Hu, C.-H.; Schaefer, H. F., III. *J. Phys. Chem.* **1993**, *97*, 10681. (b) Collins, C. L.; Meredith, C.; Yamaguchi, Y.; Schaefer III, H. F. *J. Am. Chem. Soc.* **1992**, *114*, 8694. (c) DeLeeuw, B. J.; Fermann, J. T.; Xie, Y.; Schaefer, H. F. *J. Am. Chem. Soc.* **1993**, *115*, 1039.
(7) Apeloig, Y.; Schrieber, R.; Stang, P. J. *Tetrahedron Lett.* **1980**, *21*, 411.
(8) Modarelli, D. A.; Ichimura, A. S. Unpublished data.
(9) Ervin, K. M.; Ho, J.; Lineberger, W. C. *J. Chem. Phys.* **1989**, *91*, 5974. Also see the following for information on the corresponding work with difluorovinylidene: Gilles, M. K.; Lineberger, W. C.; Ervin, K. M. *J. Am. Chem. Soc.* **1993**, *115*, 1031.
(10) Jacobson, M. P.; Silbey, R. J.; Field, R. W. *J. Chem. Phys.* **1999**, *110*, 845. Chen, Y.; Jonas, D. M.; Kinsey, J. L.; Field, R. W. *J. Chem. Phys.* **1989**, *91*, 3976.

10.1021/jo001464i CCC: $20.00
Published on Web 12/15/2000

propadienylidene (**2**) and propynylidene (**3**). McMahon et al.[12] cleanly generated **2** by direct photolysis of propynylidene (generated from diazopropyne) in an argon matrix. Identification of **2** was determined by its C═C stretch at 1952 cm^{-1}. Recently, Stanton, McMahon, and co-workers[13] were able to deconvolute the transitions in the complex absorption spectrum of **2** using the equation-of-motion coupled-cluster method (EOMEE-CCSD/TZ2P).

Difluorovinylidene (**4**) was recently observed by Sander et al.,[14] generated by irradiation of 1,2-difluoroacetylene in an argon matrix. The stability of **4** relative to **1** (R = D) was attributed to a high barrier to 1,2-F migration (i.e., 35−40 kcal mol^{-1} vs ∼3 kcal mol^{-1}).[6c,14] The IR spectrum recorded for **3** revealed an intense absorption at 1267 cm^{-1} that was assigned to the asymmetric CF_2 stretch (ν_4, b_1) vibrational state coupled by Fermi resonance to the 1245 cm^{-1} absorption ($\nu_2+\nu_5$, b_1). Significant to the work presented here, Sander and co-workers reported a second intense vibration at 1672 cm^{-1} that could be assigned to the ν_1 C═C stretch. The carbene was trapped with CO and N_2, yielding stable products that decomposed upon further irradiation.[14]

Condensed phase (solution, solid state) spectroscopy has not been performed at all on simple alkylvinylidenes such as **5**. The lack of spectroscopic evidence is a direct result of the lack of a suitable precursor for photochemical generation. Typical carbene precursors such as diazirines and diazo compounds either are not stable or do not form, although attempts have been made to synthesize these precursors.[15,16] Peroxyesters represent potentially useful precursors for the generation of alkylvinylidenes, however. Such precursors have previously been used as both thermal[11] and photochemical[17,18] sources of carbenes. Chapman and Adam[18] irradiated the cyclic peroxyester **7** at 77 K in a glassy matrix and observed production of α-lactone **8**. Upon further irradiation, these lactones were found to extrude CO, resulting in ketone formation and in one case (**8b**) loss of CO_2 to yield allene,

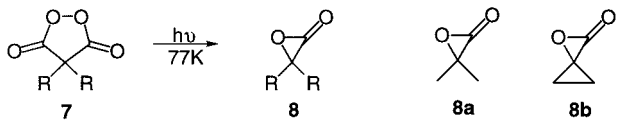

7 **8** **8a** **8b**

presumably through a carbene intermediate. Similarly, acyclic peroxide precursors have also been used as carbene precursors.[11] Thus, irradiation of *tert*-butylperoxyesters produces CO_2 and *tert*-butoxy radicals, the latter of which can undergo α-cleavage to produce methyl radicals and acetone.[19]

In this work we report the use of a peroxyester precursor to generate and observe the matrix-isolation IR spectrum of **5**. In addition we have performed a detailed theoretical interpretation of these results and of the potential energy surface (PES) of the possible rearrangement products of **5**. The information presented here represents, to the best of our knowledge, the first spectroscopic study of a dialkylvinylidene.

Experimental Section

Computational Methodology. Geometry optimizations were performed at the Hartree−Fock level with the 6-31G(d) basis set, as well as by using Becke's gradient corrected (original[20] and three-parameter[21]) exchange functionals with the correlation functional of Lee, Yang, and Parr[22] (BLYP and B3LYP, respectively[23]) with both the 6-31G(d) and 6-311G-(2d,p) basis sets. Single point energies were computed at the B3LYP/cc-pVTZ//B3LYP/6-31G(d), BLYP/cc-pVTZ//BLYP/6-31G(d), and CCSD(T)/cc-pVTZ//B3LYP/6-31G(d) levels. When used with the 6-31G(d) basis set, the DFT functionals have been shown to give excellent agreement with both experiment[24] and higher levels of theory.[24,25] DFT methods are also known to recover some electron correlation. Transition state structures were located using the synchronous transit-guided quasi-Newton (STQN) method developed by Peng and Schlegel[26] and were performed at the B3LYP/6-31G(d) level. IRC calculations were performed at the B3LYP/6-31G(d) level. All calculations were performed with the Gaussian94[27] and Gaussian98[28] sets of programs. Molecular orbitals were visualized using MacMolPlt[29] and calculated with MacGAMESS.[30] Imaginary vibrations were observed using an animation program.

Matrix-Isolation Experiments. The APD matrix isolation apparatus has been described earlier.[31] In general, the liquid

(11) Maier, G.; Reisenauer, H. P.; Schwab, W.; Cársky, P.; Hess, B. A., Jr.; Schaad, L. J. *J. Am. Chem. Soc.* **1987**, *109*, 5183. Maier, G.; Preiss, T.; Reisenauer, H. P.; Hess, B. A., Jr.; Schaad, L. J. *J. Am. Chem. Soc.* **1994**, *116*, 2014.

(12) Seburg, R. A.; Patterson, E. V.; Stanton, J. F.; McMahon, R. J. *J. Am. Chem. Soc.* **1997**, *119*, 5847−5856.

(13) Stanton, J. F.; DePinto, J. T.; Seburg, R. A.; Hodges, J. A.; McMahon, R. J. *J. Am. Chem. Soc.* **1997**, *119*, 429.

(14) Breidung, J.; Bürger, H.; Kötting, C.; Kopitzky, R.; Sander, W.; Senzlober, M.; Thiel, W.; Willner, H. *Angew. Chem., Int. Ed. Engl.* **1997**, *36*, 1983.

(15) Newman, M. S.; Okorodudu, A. O. M. *J. Org. Chem.* **1969**, *34*, 1220. Stang, P. J. *Chem. Rev.* **1978**, *78*, 383.

(16) Other photochemical precursors can be found in the following: Gilbert, J. C.; Weerasooriya, U.; Giamalva, D. *Tetrahedron Lett.* **1979**, *48*, 4619. Gilbert, J. C.; Luo, T. *J. Org. Chem.* **1981**, *46*, 5237. Gilbert, J. C.; Butler, J. R. *J. Am. Chem. Soc.* **1970**, *92*, 7493.

(17) Adam, W.; Rucktäschel, R. *J. Chem. Phys.* **1971**, *93*, 557.

(18) Chapman, O. L.; Wojtkowski, P. W.; Adam, W.; Rodriguez, O.; Rucktäschel, R. *J. Am. Chem. Soc.* **1972**, *94*, 1365−1367.

(19) Thelen, M.-A.; Felder, P.; Frey, J. G.; Huber, J. R. *J. Phys. Chem.* **1993**, *97*, 6220.

(20) Becke, A. D. *Phys. Rev. A* **1988**, *38*, 3098.

(21) Becke, A. D. *J. Chem. Phys.* **1993**, *98*, 5648.

(22) Lee, C.; Yang, W.; Parr, R. G. *Phys. Rev. B* **1988**, *37*, 785.

(23) A description of the Gaussian implementation of density functionals can be found in the following: Johnson, B. G.; Gill, P. M. W. L.; Pople, J. A. *J. Chem. Phys.* **1993**, *98*, 5612.

(24) Matzinger, S.; Bally, T.; Patterson, E. V.; McMahon, R. J. *J. Am. Chem. Soc.* **1996**, *118*, 1535−1542.

(25) Schreiner, P. R.; Karney, W. L.; von R. Schleyer, P.; Borden, W. T.; Hamilton, T. P.; Schaefer, H. F., III. *J. Org. Chem.* **1996**, *61*, 7030−7039.

(26) Peng, C.; Schlegel, H. B. *Isr. J. Chem.* **1993**, *33*, 449.

(27) Frisch, M. J.; Trucks, G. W.; Schlegel, H. B.; Gill, P. M. W.; Johnson, B. G.; Robb, M. A.; Cheeseman, J. R.; Keith, T.; Petersson, G. A.; Montgomery, J. A.; Raghavachari, K.; Al-Laham, M. A.; Zakrzewski, V. G.; Ortiz, J. V.; Foresman, J. B.; Cioslowski, J.; Stefanov, B. B.; Nanayakkara, A.; Challacombe, M.; Peng, C. Y.; Ayala, P. Y.; Chen, W.; Wong, M. W.; Andres, J. L.; Replogle, E. S.; Gomperts, R.; Martin, R. L.; Fox, D. J.; Binkley, J. S.; Defrees, D. J.; Baker, J.; Stewart, J. P.; Head-Gordon, M.; Gonzalez, C.; Pople, J. A. *Gaussian 94*, Rev. E.2; Gaussian, Inc.: Pittsburgh, PA, 1995.

(28) Frisch, M. J.; Trucks, G. W.; Schlegel, H. B.; Scuseria, G. E.; Robb, M. A.; Cheeseman, J. R.; Zakrzewski, V. G.; Montgomery, J. A., Jr.; Stratmann, R. E.; Burant, J. C.; Dapprich, S.; Millam, J. M.; Daniels, A. D.; Kudin, K. N.; Strain, M. C.; Farkas, O.; Tomasi, J.; Barone, V.; Cossi, M.; Cammi, R.; Mennucci, B.; Pomelli, C.; Adamo, C.; Clifford, S.; Ochterski, J.; Petersson, G. A.; Ayala, P. Y.; Cui, Q.; Morokuma, K.; Malick, D. K.; Rabuck, A. D.; Raghavachari, K.; Foresman, J. B.; Cioslowski, J.; Ortiz, J. V.; Stefanov, B. B.; Liu, G.; Liashenko, A.; Piskorz, P.; Komaromi, I.; Gomperts, R.; Martin, R. L.; Fox, D. J.; Keith, T.; Al-Laham, M. A.; Peng, C. Y.; Nanayakkara, A.; Gonzalez, C.; Challacombe, M.; Gill, P. M. W.; Johnson, B.; Chen, W.; Wong, M. W.; Andres, J. L.; Gonzalez, C.; Head-Gordon, M.; Replogle, E. S.; Pople, J. A. *Gaussian 98*, Rev. A.6; Gaussian, Inc.: Pittsburgh, PA, 1998.

(29) Bode, B. M.; Gordon, M. S. *J. Mol. Graphics Modell.* **1998**, *16*, 133.

(30) Schmidt, M. W.; Baldridge, K. K.; Boatz, J. A.; Elbert, S. T.; Gordon, M. S.; Jensen, J. H.; Koseki, S.; Matsunaga, N.; Nguyen, K. A.; Su, S. J.; Windus, T. L.; Dupuis, M.; Montgomery, J. A. *J. Comput. Chem.* **1993**, *14*, 1347.

(31) See, for example, the following: Bally, T. In *Radical Ionic Systems (Topics in Molecular Organization and Engineering)*; Lund, A., Shiotani, M., Eds.; Kluwer: Dordrecht, 1991; Vol. 6, pp 3−54.

Table 1. Relative Energies (in kcal/mol) of Dimethylvinylidene (5) Singlet and Triplet States by Different Quantum Chemical Methods[a]

method	5S	5T	ΔE_{ST}
HF/6-31G(d)	−155.897782535	−155.826004495[b]	45.0
MP2/6-31G(d)	−155.325245973	−155.251702809[c]	46.1
MP2/6-311+G(2d,p)	−155.459868284	−155.381212492[c]	49.4
BLYP/6-31G(d)	−155.808033637	−155.735447255[d]	45.5
BLYP/6-311+G(2d,p)	−155.864446076	−155.788282013	47.8
BLYP/cc-pVTZ//BLYP/6-31G(d)	−155.873120493	−155.792895414	50.3
B3LYP/6-31G(d)	−155.897782536	−155.826420731	44.8
B3LYP/6-311+G(2d,p)	−155.950018034	−155.874954653	47.1
B3LYP/cc-pVTZ//B3LYP/6-31G(d)	−155.959075875	−155.884580361	46.7
CCSD(T)/cc-pVTZ//B3LYP/6-31G(d)	−155.602948790	−155.530680150	45.3

[a] All structures corresponded to minima. [b] Spin contamination for this spin state was 2.397. [c] Spin contamination for this spin state was ∼2.33−2.34. [d] Values of ∼2.03−2.05 were obtained at all DFT levels.

precursor was stored in a special U-type glass tube at room temperature and connected to an argon line and a vacuum chamber. To deposit the sample on the IR salt plate, ultrahigh purity argon was passed through the U-tube, and the gaseous mixture of the precursor and argon was deposited at 14 K on the surface of a CsI window within the closed-cycle cryogenic system. The argon matrix was kept at 14 K during photolysis. UV−vis spectra were measured using a Lambda 6 UV−vis spectrophotometer, and IR spectra were recorded on a Perkin-Elmer 2000 FT-IR spectrometer with 2 cm^{-1} resolution. Precursor irradiation was performed using a Rayonet photoreactor with 254 nm bulbs.

Synthesis. 1. General. NMR spectra were recorded on a Varian Gemini-300BB NMR spectrometer in $CDCl_3$, unless reported otherwise, and are reported in ppm (δ) downfield from TMS. Infrared spectra were measured on a Perkin-Elmer 1605 FT-IR spectrometer. Melting points were obtained on either a Mel-Temp or Thomas-Hoover melting point apparatus in open capillary tubes and are uncorrected. Solvents (Aldrich or Fisher, reagent grade) were used as received unless otherwise specified.

2. Isopropylidene Malonic Acid. A two-necked 100 mL round-bottom flask was charged with KOH (2.3414 g, 0.042 mol) in a solution of 95% ethanol (5.0 mL) and water (1.5 mL). To this stirred solution, diethyl isopropylidene malonate (2.00 g, 0.010 mol) in 10 mL ethanol was added dropwise under nitrogen, and the resulting solution was refluxed overnight. Upon cooling to 0 °C, concentrated HCl was added, making sure the temperature in the reaction flask never went above 0 °C, until a pH of 4 was reached. This solution was extracted with ether, and the ether layers were dried over $MgSO_4$ and evaporated under reduced pressure to yield a yellow solid. Recrystallization of the yellow solid from chloroform afforded a white solid (0.605 g, 42%; mp 168 °C, lit. 169 °C):[32] ^{1}H NMR (acetone-d_6, δ) 1.99 (s); ^{13}C NMR (acetone-d_6, δ) 22.47, 125.81, 153.43, 166.57, 206.30; IR (1715 cm^{-1}).

3. Isopropylidene Malonyl Chloride. To a 50 mL round-bottom flask containing 0.2917 g of isopropylidene malonic acid was added ∼20 mL of $SOCl_2$, and the reaction was allowed to stir overnight under N_2 at room temperature. The excess $SOCl_2$ was removed under vacuum, leaving behind a yellow oil (0.2919 g, 79.7%). The oil was dissolved into pentane in a preweighed vial, transferred to the reaction flask, and used without purification: ^{1}H NMR ($CDCl_3$, δ) 2.16 (s); IR (1772 cm^{-1}).

4. *tert*-Butyl Isopropylidene Perester. Isopropylidene malonyl chloride (0.2919 g, 0.00161 mol) was dissolved in pentane and cooled under N_2 to 0 °C with the use of a cryocooler. To this solution was added dropwise over a 2 h period a pentane solution of 90% *tert*-butyl hydroperoxide (0.4103 g, 0.00455 mol) and pyridine (0.3602 g, 0.00455 mol). The addition caused the coloration of the clear solution to become orange, and the temperature was cooled to −30 °C and stirred for 3 days. The reaction mixture was then filtered to remove pyridinium hydrochloride and washed with 10% HCl, saturated $NaHCO_3$, and distilled water. The organic layer was dried over Na_2SO_4, filtered, and evaporated under reduced pressure to yield a colorless oil (0.1526 g, 32.8%). Purification was accomplished by column chromatography (30% ethyl acetate/hexane): ^{1}H NMR ($CDCl_3$, δ) 2.14 (s), 1.34 (s); ^{13}C NMR (acetone-d_6, δ) 23.68, 26.12, 38.68, 68.11, 84.13, 117.55, 161.40; IR (1776 cm^{-1}).

(32) Meyenberg, J. *Chem. Ber.* **1895**, *28*, 786.

Results and Discussion

Spin-state analyses of simple vinylidenes (i.e., **1**, R = H) have indicated the singlet state is substantially more stable than the triplet.[6] Previous computational studies regarding vinylidene spin states did not include alkyl substitution (i.e., **5**), so we decided to investigate the effects of alkyl substitution. Three possible conformations of **5** were thus considered: (1) an "out−out" C_{2v} geometry where the in-plane hydrogens face away from one other and toward the carbene carbon (exo to the CH_3-C-CH_3 bond angle); (2) an "in−out" C_s geometry where one methyl group was rotated 180° so that one C−H bond points inward and one outward; and (3) an "in−in" C_{2v} geometry where both in-plane C−H bonds point inward toward one another.

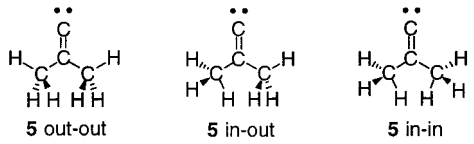

The C_s "in−out" geometry was found at all theoretical levels to have one imaginary vibration corresponding to a rotation of one methyl group, and the C_{2v} "in−in" geometry was found to have two imaginary vibrations. One vibration corresponds to a "conrotatory" double rotation and the second corresponds to a "disrotatory" double rotation, both vibrations leading to the C_{2v} "out−out" structure. All calculations were therefore performed with the C_{2v} "out−out" geometry, which was found to correspond to a minimum (i.e., no imaginary frequencies) on the potential energy surface at all levels of theory. Relative energies of the optimized out−out singlet and triplet carbenes **5S** and **5T** were computed at the Hartree−Fock, Møller−Plesset, density functional, and coupled-cluster (CCSD(T)) levels and are tabulated in Table 1.

Consistent with previous calculations,[6] we find a strong preference (∼45−50 kcal mol^{-1}) for the singlet state at all levels of theory used in the spin-state calculations. The basis for this preference is the energetic difference between the occupied orbitals in the two states. The HOMO in the singlet state is localized on the carbene

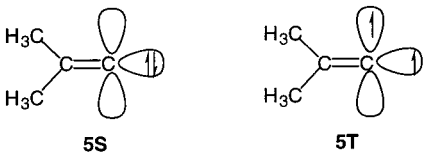

Figure 1. An orbital diagram showing the in-plane unhybridized p-orbital and the sp-hybridized orbital, at the carbene carbon atom, in **5S** and **5T**. Hyperconjugation is found to be more important to the singlet state than the triplet.

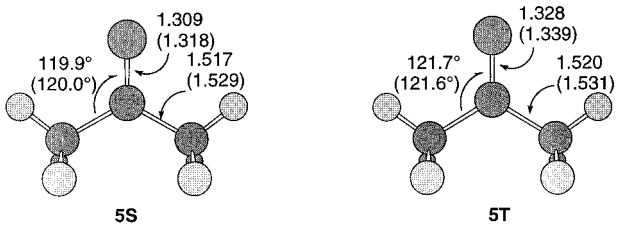

Figure 2. Bond lengths and $C_2-C_1-C_{3/4}$ bond angle for carbenes **5S** and **5T**. The values given are for geometries calculated at the B3LYP/6-31G(d) and BLYP/6-31G(d) (in parentheses) levels of theory. Bond lengths are given in angstroms and are indicated in the figure by full arrows; bond angles are indicated using half-arrows.

carbon and is sp-hybridized. The LUMO is also localized on the carbene carbon and is an unhybridized p-orbital, oriented in the molecular plane (Figure 1). This electronic arrangement is different from "typical" carbenes due to the change in the nature of the occupied nonbonding orbital from sp^2-hybridization to sp-hybridization. This change results in a lower energy HOMO for vinylidenes relative to normal carbenes, and a subsequent change in the relative energies of the HOMO and LUMO. Thus, the doubly occupied HOMO in the singlet is substantially lower in energy than the unoccupied p-orbital. In the triplet state both of these orbitals are occupied, and placement of one of the electrons into the p-orbital substantially increases the energy of this state relative to the singlet.

Increasing basis set size results in small increases in ΔE_{ST} (Table 1). This basis set effect probably results from the interaction in the singlet state of the unhybridized p-orbital on the carbene carbon with the H_3C-C σ-bonds by hyperconjugation. No similar interaction is observed in the triplet state. Increasing the amount of electron correlation, on the other hand, has the opposite effect and lowers the triplet state relative to the singlet. The effect is only slight, however, and probably is a result of the fact that electron-correlation effects are most important when the electrons are delocalized over several atoms in the molecule. Because the only pi-bond in the molecule (the C=C bond) is orthogonal to the unhybridized p-orbital, delocalization is not possible and large contributions to the energies of the singlet and triplet states are not expected with increasing correlation. Thus, only a small change in the relative energies is observed going from HF/6-31G(d) to CCSD(T)/cc-TZP//B3LYP/6-31G(d).

The singlet and triplet carbenes differ primarily in the C=C bond length due to the different occupancies of the unhybridized p-orbital (Figure 2). Singlet **5S** shows a slightly shorter C=C bond distance of 1.309 Å compared to 1.328 Å in the triplet, consistent with either a hyperconjugative stabilization between the $C-CH_3$ σ-orbitals and the empty p-orbital in the singlet state or repulsion between the methyl groups and the coplanar, singly occupied p-orbital in the triplet state. The net result in either case is a shorter C=C bond in the singlet. The progression in the $C_4-C_1-C_3$ bond angles (CH_3-C-CH_3: 120.1° in the singlet and 116.6° in the triplet) is consistent with repulsion of the $C-CH_3$ bonds with the in-plane, singly occupied p-orbital in the triplet state. The change in the $C-CH_3$ bond distances is not so noticeable and is 1.517 Å for the singlet and 1.520 Å for the triplet. The larger basis set calculations at B3LYP/6-311G(2d,p) show a slightly more pronounced change, so the C=C distances are 1.297 and 1.320 Å for the singlet and triplet states, respectively. The $C_4-C_1-C_3$ bond angles are nearly equivalent to the B3LYP/6-31G(d) results and are 120.4° for the singlet and 116.4° for the triplet state.

Matrix Isolation. Diperoxyesters have been reported as thermal[11,17] and photochemical[18] precursors for carbenes, indicating these molecules might also prove to be suitable precursors for dialkylvinylidenes. Thus, we prepared diperoxyester **6** from isopropylidene diethylmalonate by the route shown in Scheme 1. Matrix-isolation experiments were performed in both argon and Nujol matrixes; similar results were obtained with both matrixes, and the results in the Ar matrixes will be discussed here. A variety of irradiation wavelengths were initially attempted using filters and a broad-band Xe arc lamp; the results reported here were acquired by lowering the displex head, after cooling to 14 K, into a Rayonet reactor containing sixteen 254 nm bulbs.

Irradiation of **6** at 14 K for 1 min in an Ar matrix results in major changes in the IR spectrum (Figure 3). Precursor depletion is predominantly noted at 1776, 1179, 1078, and 1003 cm^{-1}, corresponding to the precursor C=O, C−O, C=C, and C=C stretches, respectively. New absorptions in the spectrum are observed at 2340, 2139, 2124, 2102, 1924, 1721, 1695, 1473, 1457, 1363, 1148, 1121, 1050, 663, and 651 cm^{-1}. Increasing the irradiation time to 5 min resulted in notable intensity increases in the absorptions at 2340, 2139, 2124, 2102, 1721, 1473, 1457, 1363, 1121, 663, and 651 cm^{-1}, while the absorptions at 1924, 1695, 1148, and 1050 cm^{-1} did not change. Similar changes were observed upon further irradiation (20 min) at 254 nm. No other absorptions were observed in either set of spectra.

When **6** was irradiated for 5 min with 254 nm light in an argon matrix doped with 9% CO (2139 cm^{-1}), a similar decrease in precursor intensities was observed (Figure 4). Interestingly, the number of absorption bands changed so that only absorptions at 2340, 2139, 2124 (shoulder), 2102, 1924, 1706, 1695, 1148, 1050, 665, and 651 cm^{-1} were observed. Increasing the irradiation time to 20 min resulted in an increase in the intensity of the absorptions at 2340, 2124 (shoulder), 2102, 1706, 665, and 651 cm^{-1} (Figure 4) and a decrease in the intensity of the band at 2139 cm^{-1} but did not affect the other absorptions (1924, 1695, 1148, and 1050 cm^{-1}).

Interpretation of IR Results. The IR spectra shown in Figure 3 are somewhat complicated due to the presence of the multiple photoproducts that are produced upon irradiation of **6**. From the spectra presented in Figures 3 and 4, it is clear that increasing irradiation times results in the preferential growth of certain absorptions. In particular, we found extended irradiation in an Ar matrix produced increasingly larger absorptions at 2340, 2139, 2124, 2102, 1721, 1363, 1121, 663, and 651 cm^{-1}, while increasing irradiation times in the Ar/

Scheme 1

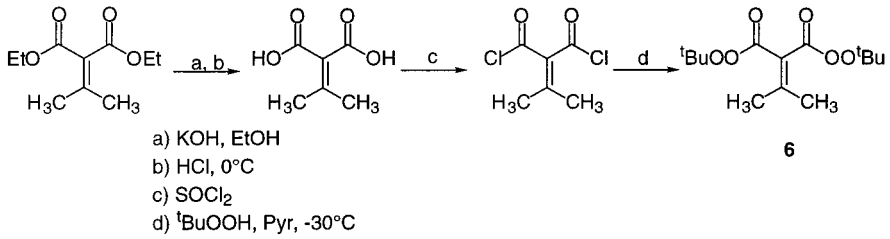

CO matrix results only in stronger signals at 2340, 2124, 2102, 1706, 663, and 651 cm^{-1}. The absorptions at 1924, 1695, 1148, and 1050 cm^{-1} did not appear to change with increasing irradiation times in either matrix. The absorption at 2340 cm^{-1} results from CO_2 in the matrix. Wentrup and Lorencak[33] have shown residual CO_2 in the displex head generally deposits on the colder parts of the displex coldfinger upon cooling to ~10 K and not on the IR windows; the presence of CO_2 on the IR windows is generally observed only during warm-up cycles. The growth of the absorption at 2340 cm^{-1} in these experiments occurs with increasing irradiation times, and its presence can therefore be attributed to the production of CO_2 during irradiation, consistent with precursor depletion. That is, irradiation of **6** results in cleavage of a peroxide bond followed by decarboxylation. The intensity of this band was shown to increase with the concomitant growth of the negative absorptions associated with precursor depletion. The absorption observed at 2139 cm^{-1} in both matrixes is due to CO. The observation that several of the absorptions increase with increasing irradiation times, while others do not, is indicative that more than one photoproduct is produced and that one or more of these photoproducts in turn undergo further photoreaction. The introductory discussion of peroxyester photochemistry and vinylidene chemistry indicates that irradiation of **6** potentially produces products **9**−**13** (Scheme 2). Due to the extremely labile nature of the precursor, and the obvious dependence of product formation on irradiation time, we performed frequency calculations at the B3LYP/6-31G(d) level to aid in deconvolution of the admittedly complicated IR spectra. These calculations, together with our rationalization of the IR spectra absorptions and a proposed mechanism for formation of the products responsible for the absorptions, are described below.

The computed vibrational frequencies and intensities of **5S** and potential photoproducts **9**−**13** are shown in Tables 2 and 3. The experimental spectrum obtained upon 254 nm photolysis of **6** in an Ar matrix (20 min) is shown together with the calculated IR spectrum of **5S** in Figure 5 (expanded to maximize the relevant spectral features). The strongest computed frequency for **5** occurs at 1701 cm^{-1}, a value that corresponds reasonably well with the observed absorption at 1721 cm^{-1} in the matrix spectrum. This absorption is consistent with the "carbonyl-like" structure of the carbene and relatively close in energy to the C═C: stretch observed for F_2C═C: by Sander et al. (1672 cm^{-1}).[14] Four of the remaining five computed frequencies have analogous absorptions in the experimental spectrum (1473, 1457, 1363, and 1121 cm^{-1} observed vs 1459, 1449, 1381, and 1055 cm^{-1} computed), although the correlation between the computed and experimental values is not as good in some cases. The absorption at 1363 cm^{-1} is quite close to the calculated absorption at 1381 cm^{-1} (a methyl group umbrella pucker), although the intensity (relative to the 1721 cm^{-1} absorption) is akin to the predicted frequencies of 1459 or 1449 cm^{-1}, while the absorption at 1120 cm^{-1} differs from the predicted IR band at 1055 cm^{-1} (an in-plane C−CH_3 symmetric rock) by 65 cm^{-1}. Nonetheless, as we will show later, these absorptions can also be attributed to **5**.

Of the remaining absorptions found in Figure 3, the absorption at 2340 cm^{-1} is readily attributed to CO_2 and that at 2139 cm^{-1} is attributed to CO. However, the absorptions observed at 2124, 2102, 1924, 1695, 1148, 1050, 663, and 651 cm^{-1} must result from either a product(s) produced from an intermediate generated *prior* to carbene formation or from reaction of the carbene through an intramolecular rearrangement or an intermolecular pathway. The possible rearrangement products methylcyclopropene (**12**) and 2-butyne (**13**) are ruled out both by frequency calculations (see Table 3) and by comparison to the published absorptions.[35,36] We have therefore identified **9**−**11** as possible sources of these absorptions. Figure 6 shows a comparison between the computed spectra for **9**−**11** with the experimentally obtained spectrum.

Chapman and Adam[18] reported formation of α-lactone **8** upon irradiation of the cyclic peroxyester **7** at 77 K. These lactones were found to have C═O absorptions in the 1895−1935 cm^{-1} region, the exact position of which depended upon the substitution at the α-carbon. Our calculations on **8a** and **8b** at the B3LYP/6-31G(d) level (Figure 7) indicate the C═O stretches occur at 1932 and 1966 cm^{-1}, respectively.

These values compare favorably with Chapman's experimental data for **8a** (1900 cm^{-1}) and **8b** (1935 cm^{-1}),[18] providing a benchmark for comparison to **9**. The IR spectra generated upon photolysis of **6** in both Ar and Ar/CO matrixes (Figures 3 and 4) show an absorption at 1924 cm^{-1} that is consistent with Chapman's observed results for the coupled C═C−C═O stretch in α-lactones. The calculated value for **9** assigned to this vibration is somewhat high at 2013 cm^{-1} but is nonetheless consistent with the trend exhibited by **8a**−**b**, for which the

(33) Wentrup, C.; Lorencak, P. *J. Am. Chem. Soc.* **1988**, *110*, 1880−1883.

(34) Wong, M. W. *Chem. Phys. Lett.* **1996**, *256*, 391−399.

(35) Butler and Newbury (Butler, I. S.; Newbury, M. L. *Spectrochim. Acta* **1980**, *36A*, 458.) have reported IR absorptions (with the corresponding relative intensities in parentheses) at 2963 (vs, br), 2925 (vs), 2862 (s), 2743 (m), 2534 (w), 2468 (w, br), 2414 (w), 2059 (m), 1840 (m), 1450 (vs, br), 1372 (m), 1251 (m, br), 1142 (s), 1037 (s, br), 803 (w), and 607 (w) cm^{-1} in the solid state (77 K).

(36) Mitchell and Merritt (Mitchell, R. W.; Merritt, J. A. *Spectrochim. Acta* **1969**, *25A*, 1881.) have reported IR absorptions (with the corresponding relative intensities in parentheses) at 3130 (w), 2960 (s), 2916 (w), 2877 (s), 1780 (m), 1478 (w), 1437 (m), 1400 (vw), 2370 (w), 1320 (vw), 1151 (m), 1093 (vw), 1056 (m), 1026 (vs), 959 (m), 921 (m), 698 (s), and 667 (w) cm^{-1} in the solid state (77 K), where w = weak, m = medium, s = strong, vs = very strong, and br = broad. See also the following: Wiberg, K. B.; Nist, B. J. *J. Am. Chem. Soc.* **1961**, *83*, 1226.

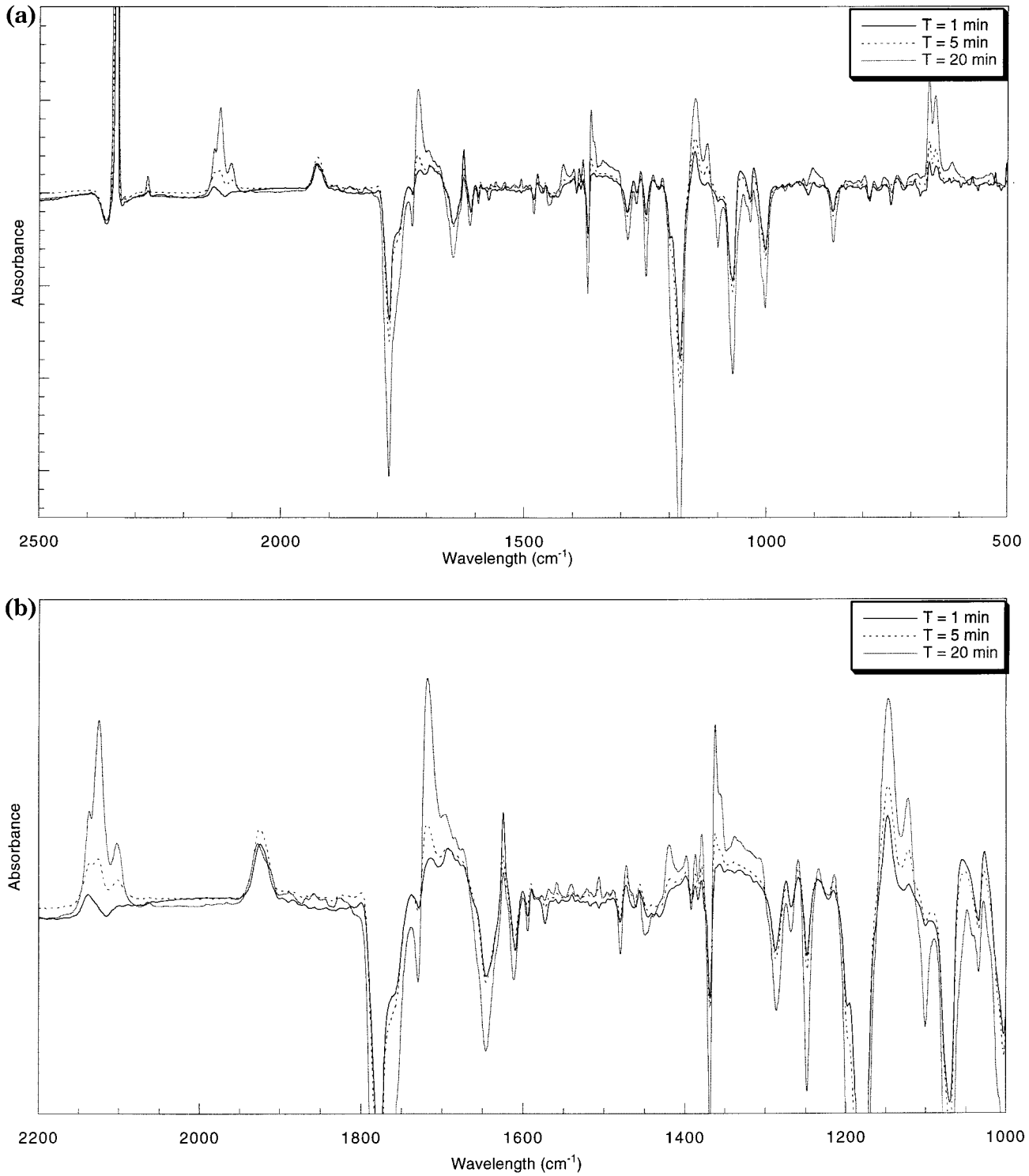

Figure 3. Experimental difference IR spectra obtained upon irradiation of **6** with 254 nm light in an Ar matrix at 14 K. Irradiation times were 1 min (a), 5 min (b) and 15 min (c); positive absorptions (up) represent growth of new absorptions, negative absorptions (down) represent precursor depletion. (a) IR spectrum from 2500 to 500 cm^{-1}. (b) IR spectrum expanded to 2200−1000 cm^{-1}.

calculated values are also high by ~30 cm^{-1}. Three other absorptions that can be attributed to **9** are observed under both matrix conditions, at 1695, 1148, and 1050 cm^{-1} (predicted: 1710, 1156, and 1051 cm^{-1}, corresponding to the C═C, asymmetric bending CH_3 mode, and an in-plane deformation of the lactone ring, respectively). The other predicted absorptions for **9** are much weaker in intensity (see Table 3) and are therefore not expected to be observed. The exception is the predicted absorption at 707 cm^{-1}, which should be comparable in intensity to the weak absorption at 1148 cm^{-1}. We do not at present have an explanation for the absence of this absorption. Two absorptions are visible at 663 and 651 cm^{-1}, but the intensity of these bands increases with increasing irradiation times. Because the intensities of the absorptions already attributed to **9** do not increase with increasing irradiation, we are not able to assign these absorptions to **9**.

Chapman et al. also demonstrated α-lactones such as **8** could undergo photodecarbonylation to yield ketones.

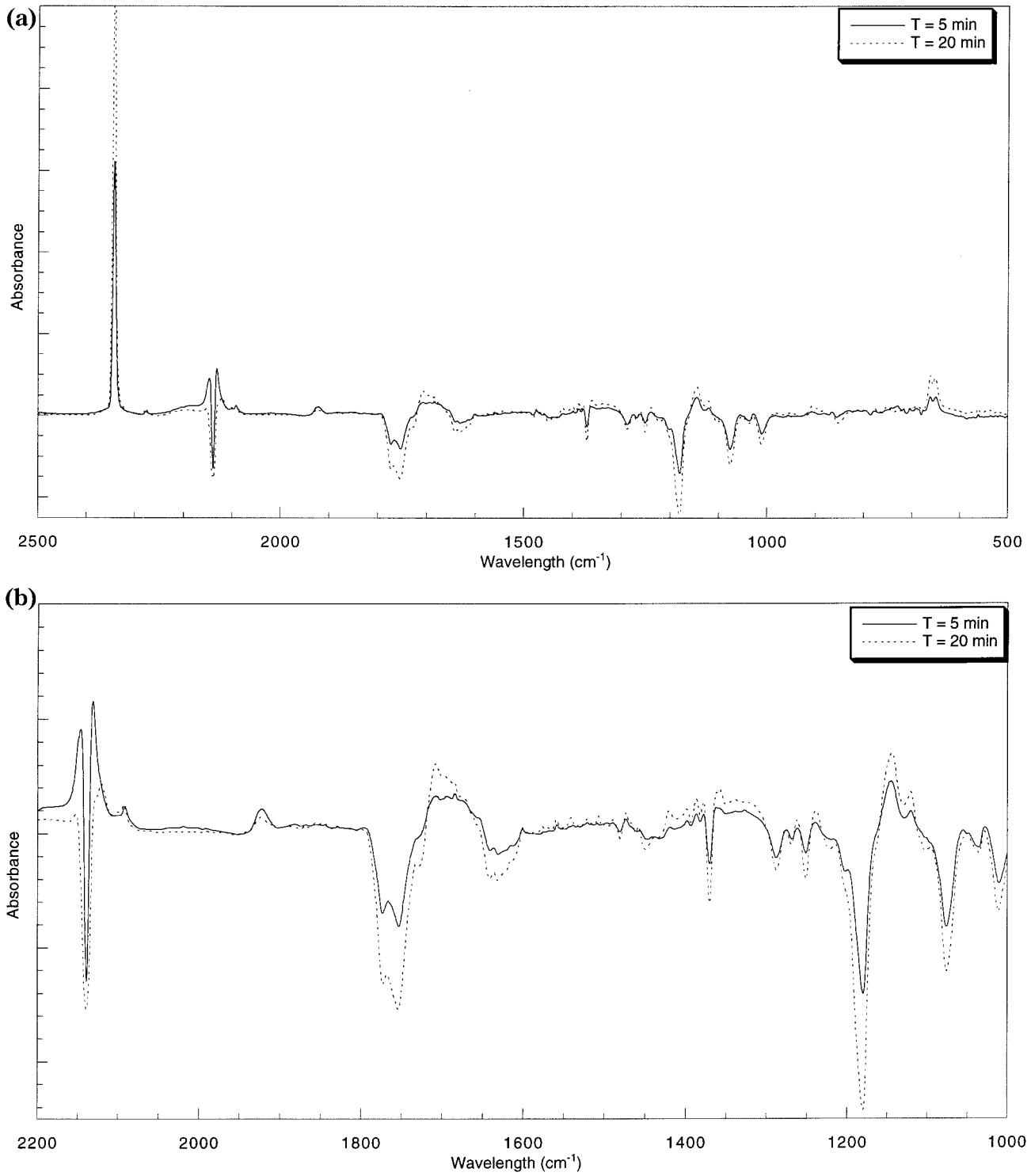

Figure 4. Experimental difference IR spectra obtained upon irradiation of **6** with 254 nm light in an Ar/CO (9% CO) matrix at 14 K. Irradiation times were 5 min (a) and 20 min (b); positive absorptions (up) represent growth of new absorptions, negative absorptions (down) represent precursor depletion. (a) IR spectrum from 2500 to 500 cm^{-1}. (b) IR spectrum expanded to 2200−1000 cm^{-1}. The absorption at 2124 cm^{-1} is observed as a shoulder growing into the 20 min spectrum. The growth of the band at 2102 cm^{-1} is minor in this particular spectrum.

The analogous reaction in α-lactone **9** is the formation of dimethyl ketene, **10**. Dimethyl ketene has an intense absorption at 2130 cm^{-1} but has only minor absorptions elsewhere.[37] Our calculated values for **10** (Table 3) are in good agreement with the experimental values. On the basis of the available experimental and computational data, we have assigned the absorption at 2102 cm^{-1} to dimethyl ketene **10**. Consistent with this observation, we have observed a growth in the signal at ∼2139 cm^{-1} in an Ar matrix with increasing irradiation times, corresponding to the loss of CO by **9** to form **10**.

(37) Parker, J.K.; Davis, S. R. *J. Phys. Chem. A* **1999**, *103*, 7280−7286. These authors have reported absorptions (with the corresponding relative intensities in parentheses) at 2902 (1.3), 2130 (100), 2065 (1.5), 1455 (0.5), 1337 (0.6), and 729 cm^{-1} (0.5).

Scheme 2

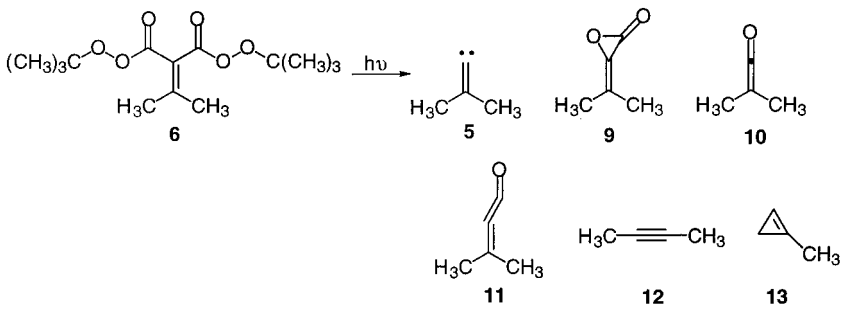

Table 2. Experimental and Calculated (B3LYP/6-31G(d)) Infrared Absorptions for Dimethylvinylidene 5

exptl[a]	calcd[b]
	3013 (12)
2973 (s)	2982 (37)
	2924 (26)
1721 (s)	1701 (36)
1473 (w)	1459 (19)
1457 (w)	1449 (13)
1363 (m)	1381 (2)
1121 (m)	1055 (10)
	762 (3)

[a] Frequencies in cm^{-1}, relative intensities in parentheses; argon matrix, 14 K. [b] Frequencies in cm^{-1} (corrected, 0.9613 scaling factor),[34] absolute intensities in parentheses.

Wentrup[33] and Dailey[38] generated dimethylpropadienone **11** under matrix-isolation conditions by flash vacuum pyrolysis. The C═C═C═O band in these experiments was reported at 2088 and 2115 cm^{-1}, respectively, and corresponds to a molecule having a bent geometry (C_s symmetry). Calculations on **11** at the B3LYP/6-31G(d) level in C_{2v} symmetry reveal a C═C═C═O absorption at 2255 cm^{-1} (scaled, one imaginary frequency at 63*i* cm^{-1}), while calculations performed within C_s symmetry (corresponding to a bent geometry) result in an absorption at 2154 cm^{-1} that corresponds reasonably well to the experimentally determined absorptions. Thus, we assign the absorption observed at 2124 cm^{-1} to **11**. The matrix data obtained previously[33,38] differs from our own by 36 and 9 cm^{-1}. The discrepancies among the three sets of results can be attributed to matrix effects. Interestingly, this absorption was found to be present in both the Ar and Ar/CO matrixes, increased in intensity in both cases with longer photolysis times, and was shown to be more intense in the Ar/CO matrix (Figure 4). Brahms and Dailey[38] reported additional weaker absorptions in their IR spectrum, at frequencies of 1777, 1765, and 1362 cm^{-1}. The frequencies calculated here for **11** are shown in Table 3 and indicate that these absorptions are expected to be less intense than the 2124 cm^{-1} absorption by at least a factor of 20. Given the intensity of signal observed by us at 2124 cm^{-1}, we are not surprised that these additional absorptions were not detected under the present conditions.

The reaction of carbenes with CO under matrix-isolation conditions has been used previously to provide evidence for carbene formation.[39,40] We reasoned that irradiation of **6** in the presence of CO should result, in addition to producing **11**, in the disappearance of the absorptions attributed to **5S**. As shown in Figure 4, the absorptions we have attributed to **5S** (1721, 1473, 1457, 1363, 1120 cm^{-1}) have completely disappeared under these conditions, while the absorption at 2124 cm^{-1} has increased. In addition, we observe a depletion of the CO peak at 2139 cm^{-1} in the IR difference spectra. These results are interpreted as evidence for the chemical trapping of **5S** and add further support for the presence of **5S** in the matrix.

One of the inevitable byproducts of *tert*-butylperoxide homolysis is the formation of the *tert*-butoxy radical, which can undergo α-cleavage and lose a methyl group to yield acetone (absorption ∼1710 cm^{-1}).[33] Because the position of our assigned C═C: stretch for **5** is at 1721 cm^{-1}, we sought to confirm that the appearance of this peak was not simply due to the presence of acetone. Literature reports[41] on the gas-phase decomposition of the *tert*-butoxy radical indicate Arrhenius parameters of logA ≈ 14.6−14.9 and E_a ≈ 15−16 kcal mol^{-1} for the C−C bond cleavage reaction. More recent results using the 248 nm output of a KrF excimer laser to generate the radical from *tert*-butyl hypochlorite in a molecular beam[42] showed E_a ≈ 20 kcal mol^{-1}, indicating a slight temperature dependence to fragmentation. Extrapolation of these results to 14 K indicates $k_{cleavage}$ should be quite small. However, the radicals generated in the molecular beam experiments were translationally hot, with enough internal energy to undergo bond cleavage. To determine whether bond cleavage to form acetone is likely under the experimental conditions used in this work, we irradiated *tert*-butylperoxide under conditions analogous to those used for irradiation of **6** (i.e., 254 nm light, 14 K, 1−30 min irradiation time). *tert*-Butylperoxide was chosen for this control experiment because its bond dissociation energy (36−39 kcal mol^{-1})[43] is close to the bond dissociation energy of *tert*-butyl benzoylperoxide (34.1 kcal mol^{-1}),[44] which is a reasonable model for **6**. The acetone carbonyl stretch generated under these conditions is found at 1715 cm^{-1} and is quite weak (Supporting Information). While this absorption is relatively close to that assigned to **5S** (1721 cm^{-1}) and was initially worrisome, we would like to point out several facts that lead us to discount formation of this molecule as being the

(38) Brahms, J. C.; Dailey, W. P. *Tetrahedron Lett.* **1990**, *31*, 1381−1384.
(39) Seburg, R. A.; McMahon, R. J. *J. Am. Chem. Soc.* **1992**, *114*, 7183.
(40) Zhu, Z.; Bally, T.; Stracener, L. L.; McMahon, R. J. *J. Am. Chem. Soc.* **1999**, *121*, 2863.
(41) Nakamura, T.; Busfield, W. K.; Jenkins, I. D.; Rizzardo, E.; Thang, S. H.; Suyama, S. *J. Org. Chem.* **2000**, *65*, 16−23. Batt, L.; Hisham, M. W. H.; Mackay, M. *Int. J. Chem. Kinet.* **1989**, *21*, 535. Heicklen, J. *Adv. Photochem.* **1988**, *14*, 177.; Batt, L.; Robinson, G. N. *Int. J. Chem. Kinet.* **1982**, *14*, 1053. Birss, F. W.; Danby, C. J.; Hinshelwood, C. *Proc. R. Soc. London, Ser. A* **1957**, *239*, 154.
(42) Thelen, M.-A.; Felder, P.; Frey, J. G.; Huber, J. R. *J. Phys. Chem.* **1993**, *97*, 6220−6225.
(43) Cubbon, R. C. P. *Prog. React. Kinet.* **1970**, *5*, 29.
(44) Tuleen, D. L.; Bentrude, W. G.; Martin, J. C. *J. Am. Chem. Soc.* **1963**, *85*, 1938.

Table 3. Experimental[a] and Calculated[b] (B3LYP/6-31G(d)) Infrared Absorptions

9		**10**		**11**		**12**[c]	**13**[d]
exptl	calcd	exptl	calcd	exptl	calcd	calcd	calcd
	3019 (13)		3006 (20)		3042 (9)	2975 (33)	2999 (20)
	2970 (32)		2952 (62)		3038 (12)	2918 (72)	2969 (84)
	2924 (35)		2910 (54)		2964 (27)	1452 (11)	2920 (20)
1924 (vs)	2013 (521)		2907 (31)		2919 (27)	1387 (10)	2917 (90)
1695 (m)	1710 (102)	2102 (s)	2131 (635)	2124 (s)	2154 (1252)	1042 (3)	1805 (11)
	1459 (18)		1464 (12)		1714 (19)		1496 (10)
	1452 (6)		1455 (14)		1458 (17)		1453 (8)
	1379 (3)		1396 (15)		1452 (9)		1449 (7)
1148 (w)	1156 (60)		1366 (11)		1363 (18)		1059 (11)
1050 (m)	1051 (174)		1174 (3)		1185 (62)		1039 (31)
	934 (7)		1005 (8)		686 (8)		916 (13)
	707 (53)		710 (4)		614 (20)		704 (26)
	635 (22)						
	628 (15)						

[a] Frequencies in cm^{-1}, relative intensities in parentheses; argon matrix, 14 K. [b] Frequencies in cm^{-1} (corrected, 0.9613 scaling factor),[34] absolute intensities in parentheses. [c] See ref 35 for experimental values. [d] See ref 36 for experimental values.

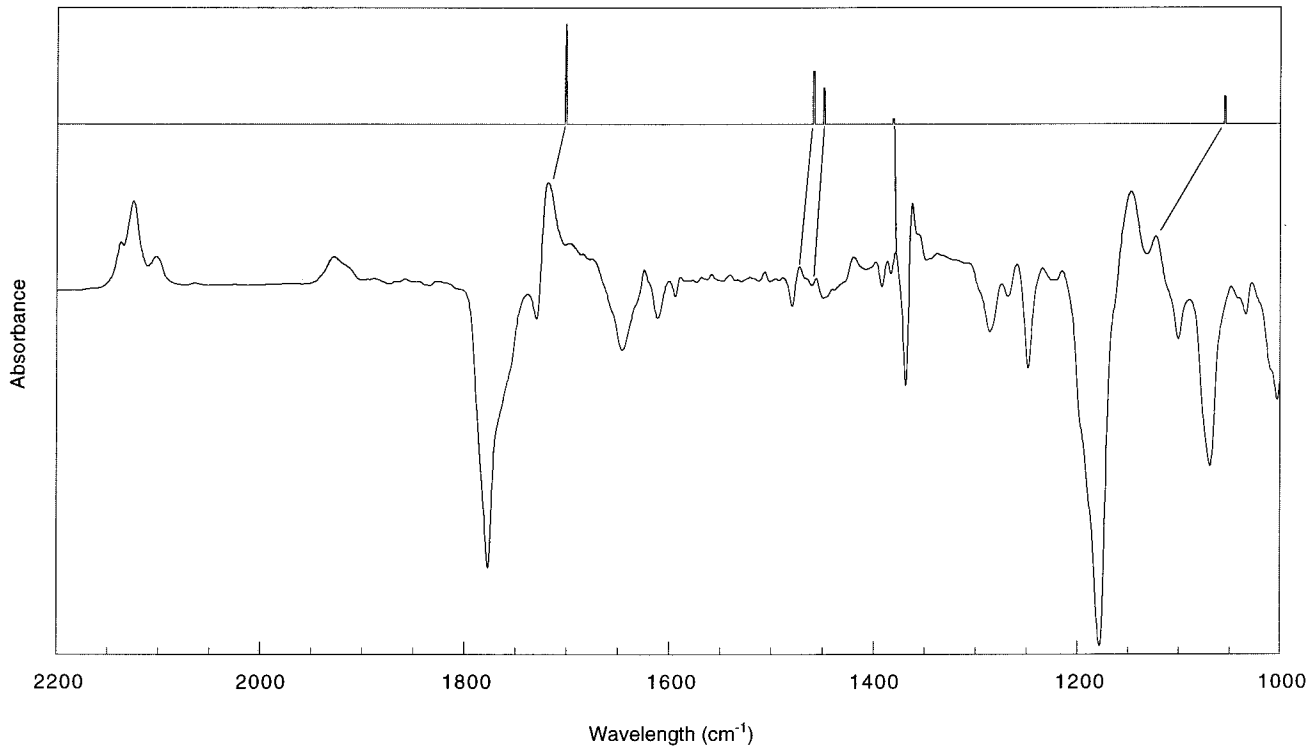

Figure 5. Comparison between the computed B3LYP/6-31G(d) IR spectrum of **5** and the experimental difference IR spectra obtained upon irradiation of **6** with 254 nm light (20 min) in an Ar matrix at 14 K.

carrier of the 1721, 1473, 1457, 1363, and 1120 cm^{-1} absorptions. First, under the irradiation conditions used in the control experiment, we observed the production of only minor amounts of acetone, despite substantial depletion of *tert*-butylperoxide (see Supporting Information). While this result at first appears surprising compared to the molecular beam experiments, α-cleavage may not be efficient under the conditions used here due to differences in the recoil energies available to each radical upon O−O vs O−Cl bond scission. Second, O−O bond scission in **6** proceeds after an initial redistribution of energy from the n→π^* excited state, and so the amount of remaining energy, that is, the internal energy available for accessing the transition state for cleavage to acetone, will be low. This reasoning necessarily implies the amount of acetone produced upon irradiation of **6** should be *less* than that observed in the control experiment. Third, the position of the carbonyl absorption is ∼5 cm^{-1} lower in energy than the band assigned to **5**, within the 2 cm^{-1} resolution of the spectrometer used in this work. Fourth, matrix EPR experiments[45] in the 12−77 K temperature range on a series of *tert*-butyl phenyl peroxyoxlates, a molecule that also yields the *tert*-butoxy radical in a mechanism similar to **6**, yielded no signals that could be identified with the characteristic signature of the methyl radical. Fifth, and most important, the spectra obtained in the Ar/CO matrix are completely devoid of absorptions in the 1710−1730 cm^{-1} region. Generation of acetone is *not* precluded by inclusion of CO in the matrix, and so if acetone is the carrier of these absorptions, these bands *should still be present* in Figure 4. The fact that we do not observe absorptions at any of these frequencies is a strong indicator that acetone is not

(45) Modarelli, D. A. Ph.D. Dissertation, The University of Massachusetts, Amherst, MA, 1991.

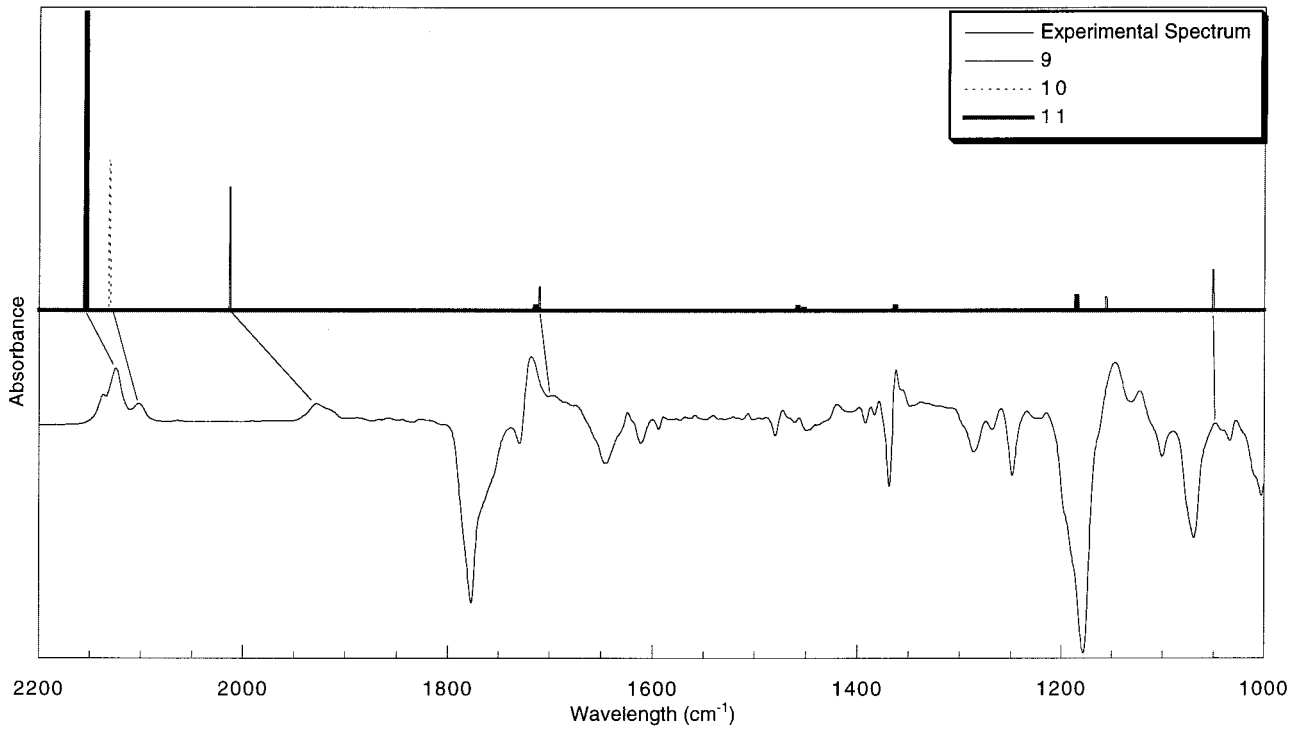

Figure 6. Comparison between the computed B3LYP/6-31G(d) IR spectra of **9**−**11** and the experimental difference IR spectra obtained upon irradiation of **6** with 254 nm light (20 min) in an Ar matrix at 14 K.

the carrier of the 1721 cm^{-1} absorption. We have observed the growth of a band at 1706 cm^{-1}, which may be due to acetone; however, if this absorption results from acetone, it is clearly not the 1721 cm^{-1} absorption we attribute to **5**.

We were somewhat surprised not to observe 2-butyne in the matrix experiments. Dailey et al.[38] identified 2-butyne as a photoproduct from irradiation at 10 K of a sample of dimethyl ketene (**10**), implying the intermediacy of **5S**. Due to the small concentration of **10** generated under the conditions used in the matrix experiments reported here, the concentration of 2-butyne may simply be too small to detect by IR.

We have not been able to positively assign several absorptions (1623, 660, and 651 cm^{-1}), either by comparison with the current literature or by comparison to computed structures.

We have thus far assigned structures **9**−**11** as the photoproducts resulting from irradiation of **6** under matrix-isolation conditions. Reaction of the carbene with the argon matrix is clearly unlikely, and so these absorptions must therefore arise from either (a) a product produced through a noncarbenic path from an intermediate generated prior to carbene formation, or (b) reaction of the carbene with CO_2 or CO (produced during irradiation of **6**). We will see that both processes occur. Irradiation (254 nm) of **6** results in preparation of an $n\rightarrow\pi^*$ excited state that leads to cleavage of the peroxide O−O bond (Scheme 3). Assuming that fragmentation of **6** is a stepwise process, the resulting acyloxyl monoradical can either (a) decarboxylate or (b) undergo a secondary O−O bond cleavage. Decarboxylation of the acyloxyl monoradical produces a vinyl monoradical (Scheme 3, path A). Scission of the second O−O peroxide bond produces an acyloxyl−vinyl diradical (**14**) that can cyclize to produce the α-lactone (**9**).

An alternative route of formation of **9** (Scheme 3, path B) involves the loss of a second *tert*-butoxy fragment from the acyloxyl monoradical prior to decarboxylation by scission of the second O−O bond. The diacyloxyl diradical generated in this process can then monodecarboxylate to yield the acyloxyl−vinyl diradical **14** and, ultimately, **9**. Regardless of the exact mechanism for formation, Chapman's work with α-lactones[18] (i.e., **8**) has indicated a sensitivity to irradiation, with decarbonylation to yield ketones a predominant path. Assuming analogous behavior to **8**, photoinduced decarbonylation of **9** produces dimethyl ketene (**10**). This result is consistent with the observed results under extended irradiation times, where we have observed little change in the absorptions attributed to **9** (1924, 1695, 1148, and 1050 cm^{-1}), while the absorption attributed to **10** (2102 cm^{-1}) and CO (2139 cm^{-1}) *increase* with increasing irradiation times. These results are internally consistent: irradiation of **6** produces a diradical intermediate that ring-closes to form lactone **9**, while irradiation of **9** produces **10**. Due to its probable instability under ambient conditions, we have not attempted to isolate **9** by another route.

On the basis of the results described above, we propose a mechanism describing the photolysis of **6** that accounts for the presence of **5** and **9**−**11** (Scheme 4). Irradiation at 254 nm produces carbene **5**, probably by first forming acyloxyl−vinyl diradical **14** upon the loss of two *tert*-butoxy radicals and CO_2. This point represents the branching point in the mechanism. Loss of CO_2 produces vinylidene **5** (Scheme 4, path A), while cyclization of the diradical produces α-lactone **9** (Scheme 4, path B). Irradiation[46] of **9** results in the loss of CO, producing dimethylketene, **10**. We suspect formation of dimethylpropadienone **11** occurs upon capture of CO from the

(46) Presumably the heat-induced loss of CO_2 occurs at higher temperatures, although we have not verified that prediction.

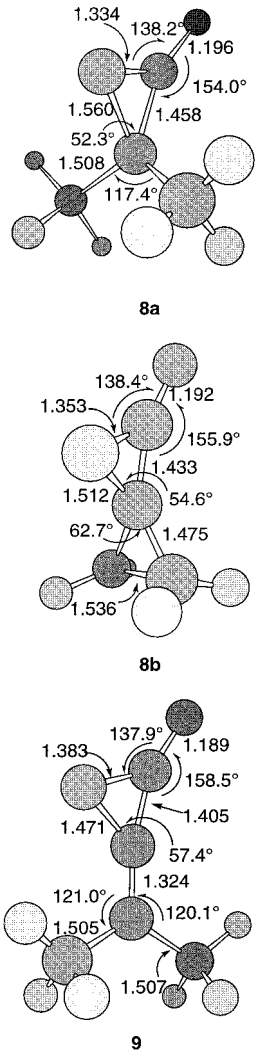

Figure 7. Bond lengths and relevant bond angles for lactones **8a**, **8a**, and **9**. The values given are for geometries calculated at the B3LYP/6-31G(d) level of theory. Bond lengths are given in angstroms and are indicated in the figure by full arrows; bond angles are indicated using half-arrows.

matrix by carbene **5** (Scheme 4, path A). When **6** is irradiated in a CO/Ar matrix, carbene **5** is trapped and observation of its IR signals suppressed. Dimethylpropadienone **11** again is the product of this trapping reaction; α-lactone **9** and dimethyl ketene **10** are produced under these conditions as well due to the different route of their formation (path B).

Comparison with Wentrup[33] and Dailey's[38] spectra indicates the absorption at 2124 cm^{-1} is due to **11**. We have been unable to rationalize the formation of this molecule from an intramolecular mechanism; however, CO is produced under the experimental conditions by photoinduced decarbonylation of **9** to form **10**. We therefore surmise the CO produced under these conditions reacts with carbene **5** to produce dimethylpropadienone, **11**.[39,40] Irradiating **6** at 14 K in an Ar matrix containing 9% CO confirms these conclusions, as the absorption assigned to **11** increases in intensity and we do not observe the absorption assigned to **5**. The mechanism of this addition is presumably similar to the addition of CO to arylcarbenes under matrix-isolation conditions.[40]

Several additional observations support the assignments of **9**−**11**. When **6** was irradiated with 254 nm light

Scheme 3

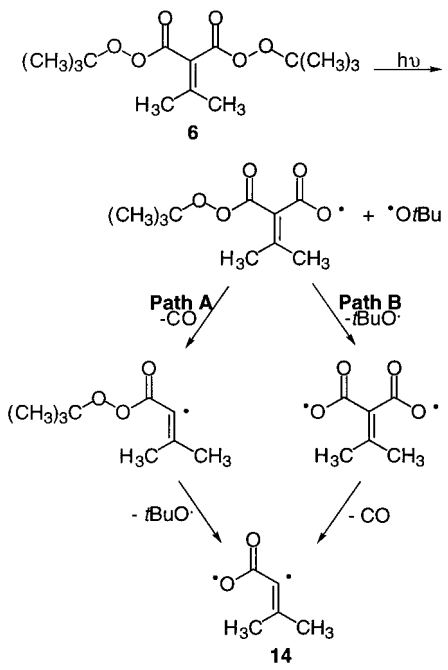

in an argon matrix doped with 9% CO, the main absorption bands observed, aside from those attributed to CO_2, were those at 1924 and 2124 cm^{-1}, consistent with formation of **9** and **11**, respectively (Table 3). Importantly, *no* IR bands consistent with **5** were observed. Because CO is known to trap carbenes under matrix-isolation conditions,[39,40] we surmise **5** is trapped to yield **11**. Formation of **9** occurs through a noncarbenic intermediate (Schemes 3 and 4), and so its formation is not precluded by the presence of CO. Assignment of the other, less intense absorptions for **9**−**11** is not possible at this time. These absorptions are all calculated to be weaker than the observed stretches by at least one order of magnitude, and therefore, these absorptions are not expected to be visible due to the low concentration of these photoproducts.

Theoretical Considerations of the Intramolecular Rearrangements of Dimethylvinylidene. The main intramolecular rearrangement pathway of vinylidene is the 1,2-H migration to form acetylene. The barrier to this rearrangement has been estimated[4,5,9] to be as high as ∼3 kcal mol^{-1} and should be quite rapid even at cryogenic temperatures. The intramolecular rearrangement products of alkylvinylidenes are expected to be similar, and alkyne formation is anticipated to be a major rearrangement product. However, the competing insertion reaction to form a cyclic alkene is also possible (Scheme 5). To address the viability of these two rearrangement pathways for **5**, we performed density functional calculations at the B3LYP/6-31G(d) level for the rearrangement of **5** to the corresponding alkyl shift (**12**) and C−H insertion (**13**) products shown in Scheme 5. The relevant structural information and relative energies of these products are shown in Figure 8 and Table 4. At the B3LYP/cc-pVTZ//B3LYP/6-31G(d) level, 2-butyne (**12**) and 1-methyl-1-cyclopropene (**13**) are more stable than **5** by ∼52 and ∼23 kcal mol^{-1}, respectively. Alkyne formation is thus a more energetically favorable intramolecular process than C−H insertion, although this result may not be general due to the strained nature of the cyclopropene ring, which is

Scheme 4

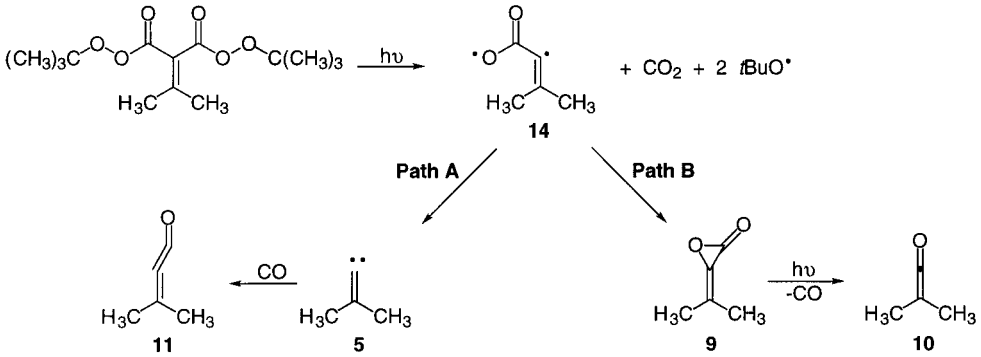

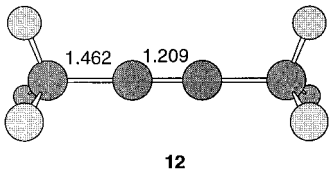

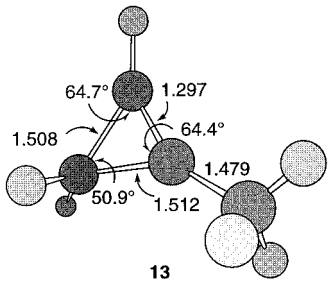

Figure 8. Bond lengths and relevant bond angles for C_4H_6 rearrangement products **12** and **13**. The values given are for geometries calculated at the B3LYP/6-31G(d) level of theory. Bond lengths are given in angstroms and are indicated in the figure by full arrows; bond angles are indicated using half-arrows.

Scheme 5

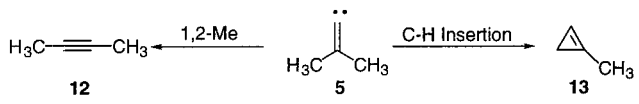

estimated using Benson equivalents[47] to be ~53.7 kcal mol^{-1} less stable than an acyclic molecule.

Given that these reactions are both substantially exothermic, it is therefore surprising that neither product was observed in any quantity in the matrix isolation experiments,[48] yet intermolecular trapping products were observed.[49] To help explain the efficient intermolecular trapping and lack of rearranged products, we examined the transition states leading to the expected rearrangement products. Transition state structures for the **5**→**12** (**TS1**) and the **5**→**13** (**TS2**) rearrangements were calculated using Schlegel's[26] STQN method, and the reaction path was followed by the IRC method. The calculated structures of **TS1** and **TS2** are shown in Figure 9. Single-point energy calculations on these structures at the B3LYP/TZP level show that **TS1** and **TS2** are 10.7 and 12.1 kcal mol^{-1} higher in energy than **5**, respectively.

Examination of **TS1** indicates an early transition state, with the migrating methyl group not quite midway along its migration axis when the transition state forms. The C−C bond undergoing scission is stretched to 1.794 Å (from 1.517 Å in the carbene), while the distance between the two carbon atoms that form the new C−C bond is 1.821 Å; importantly, the migrating carbon atom must still travel ~2.3 Å until the equilibrium 2-butyne geometry is attained. The methyl group that is not migrating forms a 166.8° angle with the forming triple bond (Figure 9). A break in symmetry from C_s to C_1 occurs along the path, resulting from methyl group rotation prior to migration. Although the migration along this path results in formation of 2-butyne with C_{2h} symmetry (the ground state is found to have C_{2v} symmetry), rotation around the C−CH_3 single bond has a nearly negligible energy barrier.[50] A second transition state ~2 kcal mol^{-1} higher in energy, and having two imaginary vibrations, was also found along the reaction path.

The transition state corresponding to C−H insertion, **TS2**, is also found rather early on the PES. **TS2** is found in C_s symmetry and exhibits a C═C bond distance of 1.322 Å, close to the 1.309 Å in **5S**, and a distance of 1.842 Å between the carbon atoms that will form the new C−C single bond. The energies of **TS1**, **TS2**, **12**, and **13** at the various computational levels used in this work are shown in Table 4.

The computational results indicate the rate constants for formation of **12** and **13** from **5** should be fairly slow at 14 K. Although this assumption is consistent with our experimental observations, it does not necessarily preclude formation of either **12** or **13** from **5**. The experimental IR spectrum obtained upon irradiation of **6** is quite complex, and the signals associated with **12** and **13** might simply be unobservable due to other absorptions. However, 2-butyne[35] has an absorption of medium intensity at 1840 cm^{-1} while 1-methylcyclopropene[36] has an absorption at 1780 cm^{-1}, also of medium intensity. Both of these absorptions occur in a region of the IR that is transparent to **5** and **9**−**11**, and we are therefore inclined to believe if either of these products is formed, it is produced in such small amounts as to preclude detection. We have argued that α-lactone **9** extrudes CO

(47) Benson, S. W.; Cruickshank, F. R.; Golden, D. M.; Haugen, G. R.; O'Neal, H. E.; Rodgers, A. S.; Shaw, R.; Walsh, R. *Chem. Rev.* **1969**, *69*, 279.

(48) The lack of the presence of the IR bands associated with methylcyclopropene and 2-butene is not necessarily proof regarding their formation. The intensity of these absorptions in the IR is not large, and so their detection in the observed spectrum is complicated by the variety of products formed during photolysis.

(49) Raman experiments were not performed on the photolyzed matrixes due to the lack of experimental facilities. Such an experiment might have enabled detection of small amounts of 2-butyne.

(50) The imaginary frequency due to methyl group rotation in C_{2h} 2-butyne is $-16i$ cm^{-1}.

Table 4. Calculated Energies of the Products Resulting from Intramolecular Rearrangement of 5[a]

compound	HF/6-31G(d)	B3LYP/ 6-31G(d)	B3LYP/cc-pVTZ// B3LYP/6-31G(d)	B3LYP/cc-pVTZ// B3LYP/6-31G(d)+ZPVE
5S	−154.8411037	−155.8977825	−155.9590759	−155.8757479
2-butyne (**12**)	−42.8	−50.9	−51.6	−50.8
TS1(**6** → **12**)	22.5	11.8	11.4	10.7
1-methylcyclopropene (**13**)	−16.9	−29.4	−28.2	−23.5
TS2 (**6** → **13**)	*b*	14.3	13.7	12.1

[a] Relative energies are shown (in parentheses) at the B3LYP/cc-pVTZ//B3LYP/6-31G(d) level of theory. [b] Geometry did not converge.

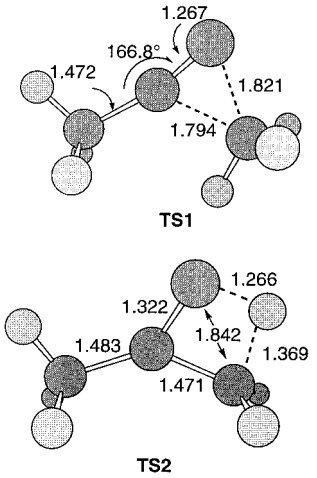

Figure 9. Bond lengths and relevant bond angles for the transition states connecting carbene **5** to rearranged products **12** and **13**. The transition states are denoted as **TS1** and **TS2**, respectively. The values given are for geometries calculated at the B3LYP/6-31G(d) level of theory. Bond lengths are given in angstroms and are indicated in the figure by full arrows; bond angles are indicated using half-arrows.

upon excitation, resulting in dimethylketene, which was used by Brahms and Dailey to produce **12** and **13**, presumably through **5**.[38] However, direct irradiation of dimethylketene should produce **5** in a vibrationally hot state that is capable of further rearrangement. Irradiation of **6**, however, probably generates **5** via a series of stepwise bond cleavages resulting in a vibrationally relaxed carbene, which does not rearrange rapidly in the matrix. We surmise dimethylketene is produced in such small quantities that loss of CO produces only minor amounts of the vibrationally hot carbene, and this amount in turn produces **12** and **13** in such small quantities so as to be undetectable.

Conclusions

Matrix-isolation irradiation of a diperoxyester precursor (**6**) in an argon matrix was used to produce dimethylvinylidene **5**, which was subsequently identified by IR spectroscopy and DFT calculations. Spin-state analysis of **5** at a variety of correlated levels indicate the singlet state is more stable than the triplet by ∼45 kcal mol^{-1}. Several additional photoproducts were identified in these experiments by correlation with their computed IR frequencies and consisted of an α-lactone (**9**), dimethylketene (**10**) and dimethylpropadienone (**11**). Neither of the expected intramolecular rearrangement products, 2-butyne or 1-methyl-1-cyclopropene, were identified in the matrix IR spectrum. DFT calculations were used to identify the potential energy surface for intramolecular rearrangement of the carbene and show a relatively high barrier to intramolecular rearrangement.

Acknowledgment. The authors would like to thank The University of Akron for their support of this work in the form of a Faculty Research Grant (FRG-1441). We would like to thank Monica Cerro-Lopez for generating the *tert*-butylperoxy radical under matrix-isolation conditions and Professor Matthew Platz (Ohio State University) for providing a critical review of the manuscript and for the use of his matrix isolation system. We would also like to thank Dr. Allan East (The University of Akron) for helpful comments on the calculations for transition state **TS1**.

Supporting Information Available: Experimental IR spectrum resulting from irradiation of *tert*-butylperoxide in an Ar matrix at 14 K, the IR difference spectrum obtained upon subtraction of the Ar and Ar/CO matrix spectra shown in Figures 3 and 4, and energies and Cartesian coordinates for **5**, **9**−**13**, and **TS1** and **TS3**. This material is available free of charge via the Internet at http://pubs.acs.org.

JO001464I